Letter

Localized states in dipolar Bose-Einstein condensates: To be or not to be of second order

A. B. Steinberg
Institut für Theoretische Physik, Universität Münster, Wilhelm-Klemm-Strasse 9, 48149 Münster, Germany

F. Maucher*
Faculty of Mechanical Engineering, Department of Precision and Microsystems Engineering, Delft University of Technology, 2628 CD Delft, The Netherlands

S. V. Gurevich and U. Thiele
Institut für Theoretische Physik, Universität Münster, Wilhelm-Klemm-Strasse 9, 48149 Münster, Germany and Center of Nonlinear Science (CeNoS), Universität Münster, Corrensstrasse 2, 48149 Münster, Germany

(Received 12 July 2024; revised 4 March 2025; accepted 9 July 2025; published 22 August 2025)

We report the existence of localized patterned states in dipolar Bose-Einstein condensates confined to a tubular geometry. We first perform a bifurcation analysis to track their emergence in an effective one-dimensional domain and find that localized states can become the ground state in suitable parameter regions. Their existence for parameters featuring a supercritical superfluid-supersolid bifurcation shows that supercriticallity is not sufficient to conclude that the phase transition is of second order; hence, density modulations can jump rather than emerge gradually. Finally, we illustrate that localized states also exist in a three-dimensional domain.

DOI: 10.1103/13k1-rxmw

In 1938, it was found that at very low temperatures helium can be superfluid, i.e., behave like a liquid without any viscosity or shear [1,2]. About 30 years later, it was speculated whether solids, i.e., states with discrete translational symmetry, could display similar behavior [3–5]. Whereas this has not yet been confirmed for helium, Bose-Einstein condensates (BECs) emerged as an ideal platform for experiments on these so-called supersolids, which were realized in 2017 by two experimental groups using supplemental light fields additionally to a spatial trap in atomic BEC [6,7].

In contrast, dipolar BECs can form a supersolid phase without the requirement of additional fields. There, the phase is stabilized by beyond mean-field contributions [8–11] permitting the realization of dipolar droplets, first observed in Refs. [12,13], and supersolids, first observed in Refs. [14–16]. Subsequently, dipolar BECs became a unique experimental setting for studying quantum fluctuations, pattern formation, phase transitions, and supersolidity [12,14–25] accompanied by theoretical advances [10,19,26–40]. The competition between dipolar interactions, quantum fluctuations, and scattering leads to intricate nonlinear dynamics and a rich phase diagram [29,32,33,39]. In particular, the change from a superfluid to a supersolid can proceed via a first- or second-order phase transition. A second-order phase transition has been predicted to occur at a single point of the phase diagram for a two-dimensional (2D) infinite pancake geometry with 2D symmetry breaking [29] and in an extended region for a three-dimensional (3D) tubular geometry with one-dimensional (1D) symmetry breaking [30,31,35,38,41].

In the context of BECs, the order of the phase transition is usually concluded via complex time evolution and by comparing the energies of the converged states, thereby assuming that the average local density is uniform across the domain. Yet, in the context of colloidal crystallization, it has been pointed out that there is a subtlety when exploring the order of phase transitions in systems with conservation of particle number [42–44], in particular in the thermodynamic limit. Namely, when using an average density as control parameter, the detection of a supercritical bifurcation is not sufficient to conclude that the phase transition is of second order. Instead, in the bifurcation analysis, one needs to probe the occurrence of localized states, e.g., finite patterned patches embedded in a uniform background, as they represent a direct signature of the occurrence of a first-order phase transition. As we will see in more detail, such states can exist even in the case of a supercritical (primary) bifurcation between the uniform and the patterned phase (and even become ground states) because the local average density can be nonuniformly redistributed across the domain. In other words, states of different mean density may coexist if they have identical chemical potential and grand potential [43,44].

Localized states represent a common phenomenon that can be observed in various pattern forming system [42,45–49]. In the present BEC context [50,51], it refers to a configuration where a finite patch of periodically spatially modulated density (supersolid) resides in a background of uniform density (superfluid). In other words, when moving along a line through the system one first finds a perfect superfluid that

*Contact author: f.maucher@tudelft.nl

Published by the American Physical Society under the terms of the Creative Commons Attribution 4.0 International license. Further distribution of this work must maintain attribution to the author(s) and the published article's title, journal citation, and DOI.

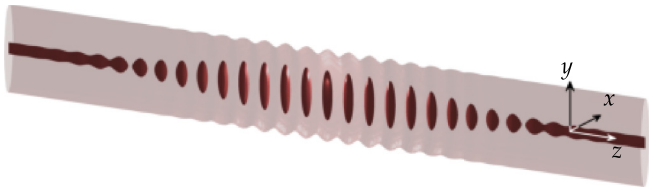

FIG. 1. Example of a stable localized state in a 3D dipolar BEC. The dipoles are polarized along the y direction; the BEC is unconfined in the z direction (axially) and tightly confined in the transverse direction. This shows that even without trap in z direction, there exist stable localized states that feature a modulated density in the central region and a perfect superfluid sufficiently far from it. Therefore, the local average density is unequally distributed across the domain. The parameters are a density of $n = 5250\,\mu\text{m}^{-1}$ and a scattering length of $a_s = 91a_0$. Contours are given at 1% (light) and 75% (dark) of the peak density. For ease of viewing, the z direction is compressed by a factor of 0.75, while the x direction is shortened due to perspective by a factor of 0.44.

then transitions via modulations of increasing amplitude into a fully modulated supersolid or droplet crystal. Figure 1 shows a numerically determined example of such a localized (stationary) state in a 3D dipolar BEC.

Although localized states were conjectured for BECs with long-range interactions [50,51], a comprehensive bifurcation analysis is to our knowledge yet to be presented for realistic long-range systems like the here considered dipolar BEC. For systems with soft-core interactions, coexistence has been discussed [52] in 2D, and arrangements of crystalline patches [53] as well as a front between the uniform and the periodic state [54] have been obtained in a 3D setting by complex time evolution, which replaces $t \to -it$ and renormalizes the wave function after each propagation step.

Here, we perform such a bifurcation analysis by way of numerical path continuation techniques [55,56] modifying the package `pde2path` [55]. In contrast to complex time evolution, this allows us to trace not only stable but also metastable and unstable uniform, periodic, and localized steady states through parameter space. We employ this for an effective 1D model that incorporates the fully nonlocal nonlinearity on domain sizes large enough to accommodate localized states. As a result, we report that localized states do indeed exist in dipolar BECs implying that the underlying phase transition is of first order.

First, we completely analyze the effective 1D system: In addition to analyzing the occurrence of localized states, we discuss their relation to the double-tangent Maxwell construction of the first-order transition [57]; i.e., we identify two states of different phase (and mean density) that have identical grand potential per particle and identical chemical potential. Second, we exemplarily show that localized states also exist in fully 3D dipolar BECs. This is only numerically feasible in a very restricted parameter range.

We consider an ensemble of N dipolar atoms of mass m at zero temperature that interact via both collisions and dipolar long-range interactions, characterized by a_s and $a_\text{dd} = m\mu_0\mu_m^2/12\pi\hbar^2$, respectively, with μ_m being the magnetic moment and μ_0 the magnetic constant. For ^{164}Dy, one has $m = 163.93$ u. The dipolar interaction is described by

$$U(r) = \frac{4\pi\hbar^2 a_s}{m}\delta(r) + \frac{\hbar^2}{m}\frac{3a_{dd}}{r^3}\left(1 - 3\frac{y^2}{r^2}\right). \tag{1}$$

Here, we assume that the dipoles are oriented along the y direction. External traps tightly confine the wave function ψ into a tubular geometry, such that the dipoles have a side-by-side orientation along the unconfined axial direction (z) and are strongly confined in the transversal directions, i.e., the polarization direction of the dipoles (y) and the remaining direction (x). Assuming equal trapping frequencies $\omega_x = \omega_y = \omega = 2\pi \times 150\,\text{Hz}$, the trapping potential is $V(\boldsymbol{r}) = V(x, y) = \omega^2(x^2 + y^2)/2$. Furthermore, the wave function is normalized to the total particle number $N = \int |\psi|^2 d^3r$.

The energy per particle is given by

$$\frac{E}{N} = \frac{1}{N}\int\left[\frac{\hbar^2}{2m}|\nabla\psi|^2 + V(\boldsymbol{r})|\psi|^2 + \frac{1}{2}|\psi|^2\int U(\boldsymbol{r}-\boldsymbol{r}')|\psi(\boldsymbol{r}')|^2 d^3r' + \frac{2}{5}\gamma_{QF}|\psi|^5\right]d^3r, \tag{2}$$

with $\gamma_{QF} = 128\hbar^2\sqrt{\pi}\sqrt{a_s}^5/3m\int_0^1 du[1+(3u^2-1)a_{dd}/a_s]^{5/2}$ [8]. To describe the dynamics, we employ the extended Gross-Pitaevskii equation that corresponds to $i\hbar\partial_t\psi = \delta E/\delta\psi^\star$ with Eq. (2).

We proceed by considering an effective 1D system with the aim of establishing that localized states must be considered when establishing the order of the phase transition: Following Ref. [31], we assume a Gaussian profile in the transverse directions that are then integrated out. More specifically, we assume $\psi(\boldsymbol{r}, t) = \psi_\parallel(z)\psi_\perp(x, y)e^{-it\mu/\hbar}$ with chemical potential μ and $\psi_\perp(x, y) = e^{-(\eta x^2+y^2/\eta)/2l^2}/\pi l$. It is useful to introduce the mean density $\bar{n} = N/L$, where L denotes the length of the tube. The 1D density is $n(z) = \int |\psi|^2 dxdy$, which in case of the transverse Gaussian profile gives $n(z) = |\psi_\parallel(z)|^2$. The parameters l and η that describe the transverse profile should be adapted when aiming at quantitative agreement. However, for localized states the optimal values of these parameters depend on position as they vary between modulated region and the uniform background (cf. Fig. 1). Therefore, we fix them as $l = 1.1456$ and $\eta = 5.8077$—corresponding to the optimal values at the primary bifurcation ($\bar{n} = \bar{n}_\text{c}$) for $a_\text{s} = 89a_0$. The effective model successfully predicts qualitative features; however, it is not fully quantitative as the actual transverse profile deviates from a Gaussian [30,31,35]. Furthermore, fixing η and l extends the region where the primary bifurcations are supercritical. The integrating-out of the transverse dimensions yields an effective 1D interaction potential of the form $\hat{U}(k) = \frac{\hbar^2}{m}\frac{2}{l^2}(a_s + a_{dd}[\frac{3Qe^Q\text{Ei}(-Q)}{\eta+1} - 1])$, where $Q = (\sqrt{\eta}k^2l^2)/2$ and $\text{Ei}(x)$ is the exponential integral function. Dimensional reduction and expansion of the quantum fluctuations [30,31] amount to $\gamma_{QF} \approx (\hbar^2/m)(256/15\pi)(a_s^{5/2}/l^3)[1 + (3a_{dd}^2/2a_s^2)]$.

The use of the resulting effective 1D model renders it numerically tractable to perform a complete bifurcation analysis using path continuation. This facilitates a complete understanding of the underlying physics. The results provide

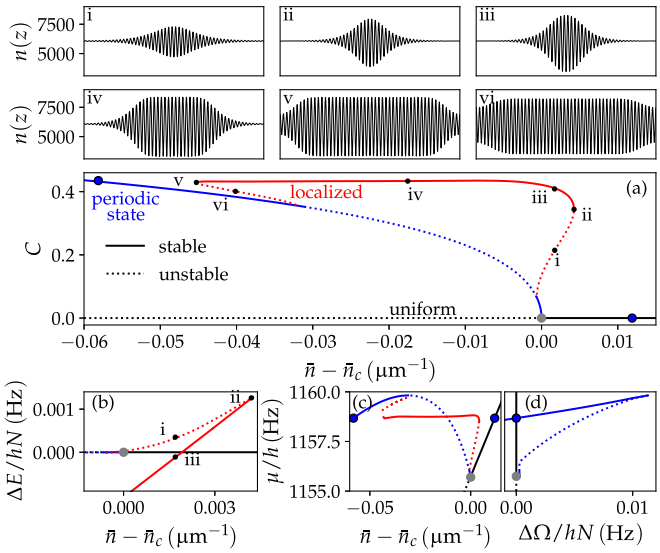

FIG. 2. Localized states in the effective 1D dipolar BEC model. Panels (a), (b), and (c) show the bifurcation diagram in terms of the contrast C, the mean energy per particle $\Delta E/N$, and the chemical potential μ, respectively, as a function of the mean density $\bar{n} - \bar{n}_c$ including branches of uniform states (black, perfect superfluid), of periodic states (blue, supersolid), and of localized states (red, coexistence). Solid (dotted) lines indicate linearly stable (unstable) states. Profiles $n(z)$ of the localized states marked i to vi in panel (a) are depicted in the top rows. The presence of localized states indicates that the superfluid-supersolid phase transition is of first order. Panel (b) indicates that the energy of the localized state is lower (e.g., state iii) than the energy of the superfluid even at densities larger than the critical one ($\bar{n}_c$, gray circle). Panel (c) clearly shows a region of constant μ indicating that the localized states represent the coexistence of different states, as further evidenced in panel (d) by the crossing of two stable branches in the $(\Delta\Omega/N, \mu)$-plane, where $\Delta\Omega/N$ is the grand potential per particle. The corresponding states are marked by filled circles in panel (a). The remaining parameters are $a_s = 89a_0$, $l = 1.1456$, and $\eta = 5.8077$.

a proof of principle that localized states exist and allow for a discussion of their general properties. Below, also a fully 3D localized state will be computed via complex time evolution. Figure 2 provides the resulting bifurcation diagram for the 1D model, which includes branches of stable, metastable, and unstable steady states for $a_s = 89a_0$ as a function of the mean density $\bar{n}$ calculated for the domain size $L = 26L_c$ with 512 grid points. Here, L_c is the modulation period. There exist steady states that are uniform (i.e., uniform in z direction), periodically modulated, i.e., with discrete translational symmetry, or localized. An upper bound for the associated superfluid fraction can be found using the Leggett estimator [5,58], which for the uniform state indicates a perfect superfluid and for the modulated state decreases with increasing modulation amplitude (not shown) [59].

Figure 2(a) presents the bifurcation diagram in terms of the contrast $C = (|\psi_\parallel|^2_{\max} - |\psi_\parallel|^2_{\min})/(|\psi_\parallel|^2_{\max} + |\psi_\parallel|^2_{\min})$ as a function of the 1D mean density $\bar{n} - \bar{n}_c$, where $\bar{n}_c = 6060.49\,\mu\mathrm{m}^{-1}$. For densities larger than $\bar{n}_c$, the uniform density state is linearly stable due to the pattern-inhibiting quantum fluctuations (black solid line). The primary bifurcation at $\bar{n} = \bar{n}_c$ (gray circle) corresponds to a symmetry-breaking supercritical pitchfork bifurcation. There, the superfluid state loses stability and a stable supersolid state featuring periodic density modulations emerges (solid blue line).

As discussed in Refs. [31,35], in the tubular geometry for assumed uniform local mean density, this phase transition can be of either first or second order, depending on the parameter region. For very small domains no localized states can develop, and in consequence, Fig. 2(a) would not contain the red line, and indicate a second-order transition. However, this does not apply for sufficiently large domains and, indeed, in the thermodynamic limit. Then, localized states do exist (red line, example profiles i to vi in top rows of Fig. 2) and can even represent the ground state(see, e.g., states iii and iv). The unstable part of the branch of localized states that represents critical nuclei bifurcates subcritically from the branch of periodic states (that also become unstable), and continues first toward higher densities while the contrast C increases. Then, at a saddle-node bifurcation (state ii) that represents a point of maximal density, the branch stabilizes and turns back toward lower $\bar{n}$. Shortly after, C reaches a plateau that continues until another limiting saddle-node bifurcation at lower $\bar{n}$ (state v). As a result, there exist extended bistable regions—one for $\bar{n} > \bar{n}_c$ between uniform and localized states and another one at lower $\bar{n}$ between localized and regular periodic states. Ultimately, after another unstable part, the branch of localized states ends on the branch of periodic states, thereby stabilizing them. Apart from the described bistable ranges, interestingly, there exists a rather extended density range where the localized states are the only stable states.

Consider now Fig. 2(b), which gives the energy difference $\Delta E = E - E_0$ between the various states and the perfectly uniform superfluid. It is interesting that state iii is the energetically most favored state even at a density that is larger than $\bar{n}_c$ where the primary bifurcation occurs (gray point). Hence, upon decreasing the density from a large value and performing complex time evolution, we first jump to state iii before reaching the primary bifurcation. This is accompanied by a jump in contrast as shown in Fig. 2(a) and, therefore, corresponds to a first-order phase transition. Figure 2(c) shows the chemical potential as a function of the density. It remains approximately constant for localized states in the range where they are stable. This is characteristic as the localized states roughly follow the line of the double-tangent Maxwell construction [57]. This applies even for finite systems, i.e., outside the thermodynamic limit [43], thereby implying that the chemical potential and the pressure (equal to the negative grand potential per particle) are identical for the coexisting phases. To better understand the origin of localized states, we furthermore consider the grand potential per particle $\Omega/N = E/N - \mu$. Usually, Ω is employed in BECs when considering finite temperature effects [37,60,61]. However, here we consider the case $T = 0$.

To thermodynamically identify coexisting phases, one checks for crossings of the superfluid and periodic state branches in the $(\mu, \Omega/N)$-plane [Fig. 2(d)]. Such a crossing indeed exists and the resulting coexisting states are marked by blue filled circles in Figs. 2(a), 2(c), and 2(d). The interval of densities between these points is where localized states can exist. The finite numerical domain results in a slightly smaller existence region.

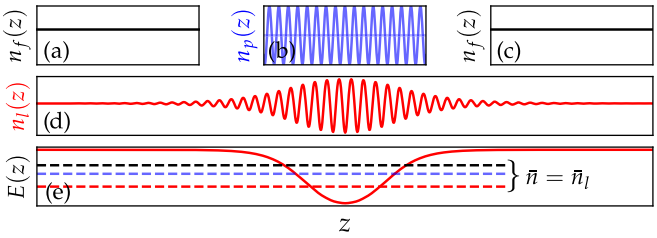

FIG. 3. Three ground states (a)–(c) that are isolated with respect to each other. The mean density of the modulated state [(b), blue] features a slightly smaller mean density, as indicated by the gray line. Removing the separating walls leads to a flux of density up to an equilibrium (d), in this case (corresponding to state iv). The ground state actually energetically prefers to retain a low-density modulated region in the center and an uniform state far from center as this is still energetically favorable as opposed to the uniform (black) and periodic states (blue) [(e), dashed lines]. The energy differences are exaggerated to dramatize the situation. The local energy of the localized state is given as a red solid line.

We would like to gain further insight as to why such states emerge. In a thought experiment visualized in Fig. 3, we imagine two boxes that each contains a different ground state, namely, a uniform (a) and a periodic state (b). The chosen states can have different mean densities. Bringing the boxes together and removing the boundaries between them, we let the system relax to a new ground state, in a simulation via complex time evolution. This leads to a flux such that finally μ becomes globally uniform. Depending on the parameters, the dynamics could crystallize the entire system, dampen out all modulations, or only smoothen the transition between the two states; i.e., the two states are pinned and form a localized state that features a local mean density that is distributed in a nonuniform fashion [cf. Fig. 3(d)]. In fact, such a configuration with nonuniform local mean density can also be energetically preferable. Consider the resulting localized state in Fig. 3: At the center of the system, the state has lower local mean density and energy per particle. In the outer parts, particle number and energy are higher. However, their combination gives a total mean energy [red horizontal line in Fig. 3(e)] that can be lower than the ones of the superfluid (black) and the periodic (blue) states.

Whereas it has been established that one has to be careful when drawing quantitative conclusions from the dimensionally reduced model [35], all of its qualitative predictions previously held and the reduction only led to a slight deformation of the phase diagram. For the sake of completeness, next we illustrate that localized states indeed also exist in the full 3D system by performing corresponding complex time evolutions for the above presented dipolar BEC model.

With Fig. 4 we contextualize the state shown in Fig. 1. The presented states are calculated with a transverse grid of 256×256 with $L_x \times L_y = 60 \times 60\,\mu\text{m}^2$. For localized states, we chose $L_z = 84\,\mu\text{m}$ and $N_z = 1792$ and otherwise $N_z = 128$ with $L_z \ll L_c$ (uniform) or $L_z = 2L_c$ (pattern). L_c is optimized by energy minimization. Again, the points of thermodynamic coexistence ($\bar{n}_{\text{coex periodic}} = 5237\,\mu\text{m}^{-1}$, $\bar{n}_{\text{coex superfluid}} = 5259\,\mu\text{m}^{-1}$) limit the density range where localized states can exist. Within this range—that is quite small in the 3D case—we are able to identify a localized state at parameters

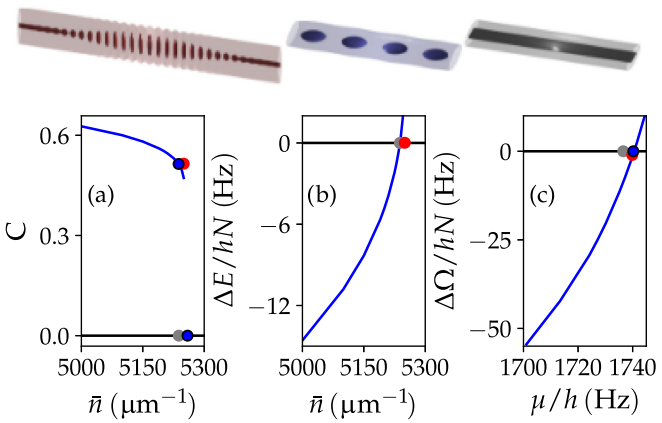

FIG. 4. Top row: Shown are example states for a 3D system with $\bar{n} = 5250\,\mu\text{m}^{-1}$, namely, a localized state (left, red), a periodic state (middle, blue), and a superfluid (right, black) with contours at 1% (light) and 75% (dark) of the peak density. For ease of viewing for the localized state (periodic and superfluid states), the z direction is compressed by a factor 0.75 [0.5]. Panel (a) displays the contrast C as a function of the mean density for supersolid state (blue), the superfluid state (black), a localized state (red dot), and the points of thermodynamic coexistence (blue rimmed dots). The gray dot indicates states at the energy crossing shown in panel (b). Panel (c) depicts the Maxwell construction and gives the coexistence points.

with a weakly subcritical primary bifurcation. Here, in the region with a supercritical primary bifurcation, the front width between patterned and uniform parts becomes too large for the present computational means.

To conclude, we have shown that localized states exist in dipolar BECs. This has a number of interesting implications when exploring the thermodynamic limit and the order of the superfluid-supersolid phase transition. First, it clarifies that the qualification of a phase transition as first or second order needs to be based either on a full bifurcation analysis including localized states in large domains (possibly computationally prohibitive) or on a treatment that allows one to assess the possibility of a Maxwell construction. Second, from the perspective of superfluidity and supersolidity, localized states are interesting as the wave function can feature a continuous transition from a perfect superfluid to a supersolid and ultimately possibly to insulating droplets in a single experimental realization in a domain of sufficient size. Although current experiments do not yet allow for the observation of localized states due to limitations of the condensed atom number, our predictions based on the effective 1D model show that experimental setups that are by a factor of 2 larger than the present ones (e.g., Ref. [23]) will be sufficiently large for an observation of metastable localized states. About a factor of 5 is needed to find them as the ground state and therefore to obtain a clear signature of a first-order phase transition. In this context, it will be interesting to explore minimal finite BECs [62]—i.e., trapped in the z direction as well—for realistic experimental parameters (limited particle number and sufficiently low density) that can support localized states. Furthermore, exploring localized states at the dimensional crossover [25] appears interesting. In addition,

a comprehensive bifurcation analysis should be devoted to the three-dimensional case once computational methods have further advanced. Furthermore, it would be interesting to add temperature fluctuations and explore their effect on localized states in dipolar BECs [37,38] and localized states in molecular BECs and their experimental feasibility [63].

We acknowledge that parts of the calculations were performed on the HPC cluster PALMA II of the University of Münster partly funded by the DFG (INST 211/667-1).

The data that support the findings of this study are openly available on [64].

[1] P. Kapitza, Viscosity of liquid helium below the λ-point, Nature (London) **141**, 74 (1938).
[2] J. F. Allen and A. D. Misener, Flow phenomena in liquid helium II, Nature (London) **142**, 643 (1938).
[3] A. F. Andreev and I. M. Lifshitz, Quantum theory of defects in crystals, Sov. Phys. JETP **29**, 1107 (1969).
[4] G. V. Chester, Speculations on Bose-Einstein condensation and quantum crystals, Phys. Rev. A **2**, 256 (1970).
[5] A. J. Leggett, Can a solid be "superfluid"? Phys. Rev. Lett. **25**, 1543 (1970).
[6] J. Léonard, A. Morales, P. Zupancic, T. Esslinger, and T. Donner, Supersolid formation in a quantum gas breaking a continuous translational symmetry, Nature (London) **543**, 87 (2017).
[7] J.-R. Li, J. Lee, W. Huang, S. Burchesky, B. Shteynas, F. Ç. Top, A. O. Jamison, and W. Ketterle, A stripe phase with supersolid properties in spin–orbit-coupled Bose-Einstein condensates, Nature (London) **543**, 91 (2017).
[8] A. R. P. Lima and A. Pelster, Quantum fluctuations in dipolar Bose gases, Phys. Rev. A **84**, 041604 (2011).
[9] A. R. P. Lima and A. Pelster, Beyond mean-field low-lying excitations of dipolar Bose gases, Phys. Rev. A **86**, 063609 (2012).
[10] F. Wächtler and L. Santos, Quantum filaments in dipolar Bose-Einstein condensates, Phys. Rev. A **93**, 061603 (2016).
[11] H. Saito, Path-integral Monte Carlo study on a droplet of a dipolar Bose–Einstein condensate stabilized by quantum fluctuation, J. Phys. Soc. Jpn. **85**, 053001 (2016).
[12] H. Kadau, M. Schmitt, M. Wenzel, C. Wink, T. Maier, I. Ferrier-Barbut, and T. Pfau, Observing the Rosensweig instability of a quantum ferrofluid, Nature (London) **530**, 194 (2016).
[13] M. Schmitt, M. Wenzel, F. Böttcher, I. Ferrier-Barbut, and T. Pfau, Self-bound droplets of a dilute magnetic quantum liquid, Nature (London) **539**, 259 (2016).
[14] F. Böttcher, J.-N. Schmidt, M. Wenzel, J. Hertkorn, M. Guo, T. Langen, and T. Pfau, Transient supersolid properties in an array of dipolar quantum droplets, Phys. Rev. X **9**, 011051 (2019).
[15] L. Tanzi, E. Lucioni, F. Famà, J. Catani, A. Fioretti, C. Gabbanini, R. N. Bisset, L. Santos, and G. Modugno, Observation of a dipolar quantum gas with metastable supersolid properties, Phys. Rev. Lett. **122**, 130405 (2019).
[16] L. Tanzi, S. M. Roccuzzo, E. Lucioni, F. Famà, A. Fioretti, C. Gabbanini, G. Modugno, A. Recati, and S. Stringari, Supersolid symmetry breaking from compressional oscillations in a dipolar quantum gas, Nature (London) **574**, 382 (2019).
[17] L. Chomaz, D. Petter, P. Ilzhöfer, G. Natale, A. Trautmann, C. Politi, G. Durastante, R. M. W. van Bijnen, A. Patscheider, M. Sohmen, M. J. Mark, and F. Ferlaino, Long-lived and transient supersolid behaviors in dipolar quantum gases, Phys. Rev. X **9**, 021012 (2019).
[18] G. Natale, R. M. W. van Bijnen, A. Patscheider, D. Petter, M. J. Mark, L. Chomaz, and F. Ferlaino, Excitation spectrum of a trapped dipolar supersolid and its experimental evidence, Phys. Rev. Lett. **123**, 050402 (2019).
[19] M. Guo, F. Böttcher, J. Hertkorn, J.-N. Schmidt, M. Wenzel, H. P. Büchler, T. Langen, and T. Pfau, The low-energy Goldstone mode in a trapped dipolar supersolid, Nature (London) **574**, 386 (2019).
[20] L. Tanzi, J. G. Maloberti, G. Biagioni, A. Fioretti, C. Gabbanini, and G. Modugno, Evidence of superfluidity in a dipolar supersolid from nonclassical rotational inertia, Science **371**, 1162 (2021).
[21] D. Petter, A. Patscheider, G. Natale, M. J. Mark, M. A. Baranov, R. van Bijnen, S. M. Roccuzzo, A. Recati, B. Blakie, D. Baillie, L. Chomaz, and F. Ferlaino, Bragg scattering of an ultracold dipolar gas across the phase transition from Bose-Einstein condensate to supersolid in the free-particle regime, Phys. Rev. A **104**, L011302 (2021).
[22] T. Ilg, J. Kumlin, L. Santos, D. S. Petrov, and H. P. Büchler, Dimensional crossover for the beyond-mean-field correction in Bose gases, Phys. Rev. A **98**, 051604 (2018).
[23] M. A. Norcia, C. Politi, L. Klaus, E. Poli, M. Sohmen, M. J. Mark, R. N. Bisset, L. Santos, and F. Ferlaino, Two-dimensional supersolidity in a dipolar quantum gas, Nature (London) **596**, 357 (2021).
[24] M. A. Norcia, E. Poli, C. Politi, L. Klaus, T. Bland, M. J. Mark, L. Santos, R. N. Bisset, and F. Ferlaino, Can angular oscillations probe superfluidity in dipolar supersolids? Phys. Rev. Lett. **129**, 040403 (2022).
[25] G. Biagioni, N. Antolini, A. Alaña, M. Modugno, A. Fioretti, C. Gabbanini, L. Tanzi, and G. Modugno, Dimensional crossover in the superfluid-supersolid quantum phase transition, Phys. Rev. X **12**, 021019 (2022).
[26] R. N. Bisset, R. M. Wilson, D. Baillie, and P. B. Blakie, Ground-state phase diagram of a dipolar condensate with quantum fluctuations, Phys. Rev. A **94**, 033619 (2016).
[27] R. Bombin, J. Boronat, and F. Mazzanti, Dipolar Bose supersolid stripes, Phys. Rev. Lett. **119**, 250402 (2017).
[28] S. M. Roccuzzo and F. Ancilotto, Supersolid behavior of a dipolar Bose-Einstein condensate confined in a tube, Phys. Rev. A **99**, 041601 (2019).
[29] Y.-C. Zhang, F. Maucher, and T. Pohl, Supersolidity around a critical point in dipolar Bose-Einstein condensates, Phys. Rev. Lett. **123**, 015301 (2019).
[30] P. B. Blakie, D. Baillie, and S. Pal, Variational theory for the ground state and collective excitations of an elongated dipolar condensate, Commun. Theor. Phys. **72**, 085501 (2020).
[31] P. Blakie, D. Baillie, L. Chomaz, and F. Ferlaino, Supersolidity in an elongated dipolar condensate, Phys. Rev. Res. **2**, 043318 (2020).

[32] Y.-C. Zhang, T. Pohl, and F. Maucher, Phases of supersolids in confined dipolar Bose-Einstein condensates, Phys. Rev. A **104**, 013310 (2021).

[33] J. Hertkorn, J.-N. Schmidt, M. Guo, F. Böttcher, K. S. H. Ng, S. D. Graham, P. Uerlings, T. Langen, M. Zwierlein, and T. Pfau, Pattern formation in quantum ferrofluids: From supersolids to superglasses, Phys. Rev. Res. **3**, 033125 (2021).

[34] J. Hertkorn, J.-N. Schmidt, M. Guo, F. Böttcher, K. S. H. Ng, S. D. Graham, P. Uerlings, H. P. Büchler, T. Langen, M. Zwierlein, and T. Pfau, Supersolidity in two-dimensional trapped dipolar droplet arrays, Phys. Rev. Lett. **127**, 155301 (2021).

[35] J. C. Smith, D. Baillie, and P. B. Blakie, Supersolidity and crystallization of a dipolar Bose gas in an infinite tube, Phys. Rev. A **107**, 033301 (2023).

[36] Y.-C. Zhang and F. Maucher, Variational approaches to two-dimensionally symmetry-broken dipolar Bose–Einstein condensates, Atoms **11**, 102 (2023).

[37] J. Sánchez-Baena, C. Politi, F. Maucher, F. Ferlaino, and T. Pohl, Heating a dipolar quantum fluid into a solid, Nat. Commun. **14**, 1868 (2023).

[38] J. Sánchez-Baena, T. Pohl, and F. Maucher, Superfluid-supersolid phase transition of elongated dipolar Bose-Einstein condensates at finite temperatures, Phys. Rev. Res. **6**, 023183 (2024).

[39] Y.-C. Zhang, T. Pohl, and F. Maucher, Metastable patterns in one- and two-component dipolar Bose-Einstein condensates, Phys. Rev. Res. **6**, 023023 (2024).

[40] G. Li, Z. Zhao, X. Jiang, Z. Chen, B. Liu, B. A. Malomed, and Y. Li, Strongly anisotropic vortices in dipolar quantum droplets, Phys. Rev. Lett. **133**, 053804 (2024).

[41] P. B. Blakie, L. Chomaz, D. Baillie, and F. Ferlaino, Compressibility and speeds of sound across the superfluid-to-supersolid phase transition of an elongated dipolar gas, Phys. Rev. Res. **5**, 033161 (2023).

[42] U. Thiele, A. J. Archer, M. J. Robbins, H. Gomez, and E. Knobloch, Localized states in the conserved Swift-Hohenberg equation with cubic nonlinearity, Phys. Rev. E **87**, 042915 (2013).

[43] U. Thiele, T. Frohoff-Hülsmann, S. Engelnkemper, E. Knobloch, and A. J. Archer, First order phase transitions and the thermodynamic limit, New J. Phys. **21**, 123021 (2019).

[44] M. P. Holl, A. J. Archer, S. V. Gurevich, E. Knobloch, L. Ophaus, and U. Thiele, Localized states in passive and active phase-field-crystal models, IMA J. Appl. Math. **86**, 896 (2021).

[45] M. Tlidi, P. Mandel, and R. Lefever, Localized structures and localized patterns in optical bistability, Phys. Rev. Lett. **73**, 640 (1994).

[46] J. Burke and E. Knobloch, Localized states in the generalized Swift-Hohenberg equation, Phys. Rev. E **73**, 056211 (2006).

[47] D. J. Lloyd, B. Sandstede, D. Avitabile, and A. R. Champneys, Localized hexagon patterns of the planar Swift–Hohenberg equation, SIAM J. Appl. Dyn. Syst. **7**, 1049 (2008).

[48] E. Knobloch, Spatial localization in dissipative systems, Annu. Rev. Condens. Matter Phys. **6**, 325 (2015).

[49] E. Knobloch, Localized structures and front propagation in systems with a conservation law, IMA J. Appl. Math. **81**, 457 (2016).

[50] V. Heinonen, K. J. Burns, and J. Dunkel, Quantum hydrodynamics for supersolid crystals and quasicrystals, Phys. Rev. A **99**, 063621 (2019).

[51] A. B. Steinberg, F. Maucher, S. V. Gurevich, and U. Thiele, Exploring bifurcations in Bose-Einstein condensates via phase field crystal models, Chaos **32**, 113112 (2022).

[52] M. Kunimi and Y. Kato, Mean-field and stability analyses of two-dimensional flowing soft-core bosons modeling a supersolid, Phys. Rev. B **86**, 060510 (2012).

[53] N. Henkel, R. Nath, and T. Pohl, Three-dimensional roton excitations and supersolid formation in Rydberg-excited Bose-Einstein condensates, Phys. Rev. Lett. **104**, 195302 (2010).

[54] F. Ancilotto, M. Rossi, and F. Toigo, Supersolid structure and excitation spectrum of soft-core bosons in three dimensions, Phys. Rev. A **88**, 033618 (2013).

[55] H. Uecker, D. Wetzel, and J. D. M. Rademacher, pde2path—A Matlab package for continuation and bifurcation in 2D elliptic systems, Numer. Math. Theor. Meth. Appl. **7**, 58 (2014).

[56] S. Engelnkemper, S. V. Gurevich, H. Uecker, D. Wetzel, and U. Thiele, Continuation for thin film hydrodynamics and related scalar problems, in *Computational Modeling of Bifurcations and Instabilities in Fluid Mechanics*, *Computational Methods in Applied Sciences*, edited by A. Gelfgat (Springer, Cham, 2019), Vol 50, pp. 459–501.

[57] H. B. Callen, *Thermodynamics* (John Wiley & Sons, Inc., New York, 1960).

[58] A. J. Leggett, On the superfluid fraction of an arbitrary many-body system at $T = 0$, J. Stat. Phys. **93**, 927 (1998).

[59] Where necessary, path continuation results are refined using complex time evolution. In the case of meta- and unstable states, data are extrapolated from neighboring results.

[60] A. Griffin, Conserving and gapless approximations for an inhomogeneous Bose gas at finite temperatures, Phys. Rev. B **53**, 9341 (1996).

[61] S. Ronen and J. L. Bohn, Dipolar Bose-Einstein condensates at finite temperature, Phys. Rev. A **76**, 043607 (2007).

[62] A. Alaña, N. Antolini, G. Biagioni, I. n. L. Egusquiza, and M. Modugno, Crossing the superfluid-supersolid transition of an elongated dipolar condensate, Phys. Rev. A **106**, 043313 (2022).

[63] N. Bigagli, W. Yuan, S. Zhang, B. Bulatovic, T. Karman, I. Stevenson, and S. Will, Observation of Bose–Einstein condensation of dipolar molecules, Nature (London) **631**, 289 (2024).

[64] A. B. Steinberg, F. Maucher, S. V. Gurevich, U. Thiele, Data supplement for 'Localized states in dipolar Bose-Einstein condensates: To be or not to be of second order', Zenodo (2025), https://doi.org/10.5281/zenodo.16778935.